Inorg. Chem. **2003**, *42*, 6024–6031

Synthesis, X-ray Diffraction Structures, Spectroscopic Properties, and in vitro Antitumor Activity of Isomeric (1*H*-1,2,4-Triazole)Ru(III) Complexes

Vladimir B. Arion,*,† Erwin Reisner,†,‡ Madeleine Fremuth,† Michael A. Jakupec,† Bernhard K. Keppler,*,† Vadim Yu. Kukushkin,§ and Armando J. L. Pombeiro‡

Institute of Inorganic Chemistry of the University of Vienna, Währingerstr. 42, A-1090 Vienna, Austria, Centro de Quìmica Estrutural, Complexo I, Instituto Superior Técnico, Av. Rovisco Pais, 1049-001 Lisbon, Portugal, and Department of Chemistry, St. Petersburg State University, 198504 Stary Petergof, Russian Federation

Received June 2, 2003

Three ruthenium(III) complexes containing 1*H*-1,2,4-triazole (Htrz), viz., $(H_2trz)[cis\text{-}RuCl_4(Htrz)_2]$, **1**, $(H_2trz)[trans\text{-}RuCl_4(Htrz)_2]$, **2**, and $(Ph_3PCH_2Ph)[trans\text{-}RuCl_4(Htrz)_2]$, **3**, have been synthesized by reaction between $RuCl_3$ and excess of the triazole in 2.38 M HCl (**1** and **2**), while **3** was obtained by metathesis of **2** and $[Ph_3PCH_2Ph]Cl$ in water. The products were characterized by IR, UV–vis, electrospray mass spectrometry, cyclic voltammetry, and X-ray crystallography (**1** and **3**). X-ray diffraction study revealed *cis* and *trans* arrangements of the triazole ligands in **1** and **3**, correspondingly, and unprecedented monodentate coordination of the triazole through N2 and stabilization of its 4*H* tautomeric form, which is the disfavored one for the free triazole. The cytotoxicity of **1** and **2** has been assayed in three human carcinoma cell lines SW480, HT29 (colon carcinoma), and SK-BR-3 (mammary carcinoma). Both compounds exhibit antiproliferative activity in vitro. Time-dependent response of all three lines to **1** and **2** and a structure–activity relationship, i.e., higher activity of the *trans*-isomer **2** than that of *cis*-species **1**, have been observed.

Introduction

The therapeutic potential of both nonphysiological and physiological metal ion complexes against tumor cells, is well documented.[1−15] Current efforts are focused to develop metal-based drugs with improved clinical effectiveness, reduced general toxicity, and a broader spectrum of activity. Among the non-platinum compounds exhibiting anticancer properties, those of ruthenium are very promising, showing activity on even such tumors which developed resistance to cisplatin or in which cisplatin is totally inactive. Moreover, in contrast to cisplatin, the toxic side effects of these Ru compounds are remarkably low.

The first ruthenium compound $(Him)[trans\text{-}RuCl_4(im)(Me_2SO)]$ (NAMI-A; im = imidazole) entered phase I clinical trials in 1999 as an antimetastatic drug,[16] whereas another complex $(Hind)[trans\text{-}RuCl_4(ind)_2]$ (KP1019; ind = indazole, Figure 1) has entered phase I clinical trials in 2003 as an anticancer drug which is very active against colon carcinomas and their metastases.[17] Another (azole)Ru(III) complex, $(Him)[trans\text{-}RuCl_4(im)_2]$, also prepared in our laboratory,

* To whom correspondence should be addressed. E-mail: arion@ap.univie.ac.at (V.B.A.); keppler@ap.univie.ac.at (B.K.K.). Fax: + 43 1 427752680.

† University of Vienna.

‡ Instituto Superior Técnico.

§ St. Petersburg State University.

(1) Rosenberg, B.; Vancamp, L. *Cancer Res.* **1970**, *30*, 1799−1802.
(2) Graham, R. D.; Williams, D. R. *J. Inorg. Nucl. Chem.* **1979**, *41*, 1245−1249.
(3) Myette, M. S.; Elford, M. L.; Chitambar, C. R. *Cancer Lett.* **1998**, *129*, 199−204.
(4) Lovejoy, D. B.; Richardson, D. R. *Expert. Opin. Invest. Drugs* **2000**, *9*, 1257−1270 and references therein.
(5) Erck, A.; Rainen, L.; Whileyman, J.; Chang, I.-M.; Kimball, A. P.; Bear, J. *Proc. Soc. Exp. Biol. Med.* **1974**, *145*, 1278−1283.
(6) Saryan, L. A.; Ankel, E.; Krishnamurti, C.; Petering, D. H.; Elford, H. *J. Med. Chem.* **1979**, *22*, 1218−1221.
(7) Booth, B.; Sartorelli, A. *Nature* **1966**, *210*, 104−105.
(8) Booth, B.; Donelly, T.; Zettner, A.; Sartorelli, A. *Biochem. Pharmacol.* **1971**, *20*, 3109−3118.
(9) Keppler, B. K.; Lipponer, K.-G.; Stenzel, B.; Kratz, F. In *Metal Complexes in Cancer Chemotherapy*; Keppler, B. K., Ed.; VCH: Weinheim, 1993; pp 187−220.
(10) Allardyce, C. S.; Dyson, P. J. *Platinum Met Rev.* **2001**, *45*, 62−69.
(11) Guo, Z.; Sadler, P. J. *Angew. Chem., Int. Ed.* **1999**, *38*, 1512−1531.
(12) Pieper, T.; Borsky, K.; Keppler, B. K. *Top. Biol. Inorg. Chem.* **1999**, *1*, 171−199.
(13) Clarke, M. J. *Coord. Chem. Rev.* **2003**, *236*, 209−233.
(14) Espósito, B. P.; Najjar, R. *Coord. Chem. Rev.* **2002**, *232*, 137−149.
(15) Sava, G.; Bergamo, A. *Int. J. Oncol.* **2000**, *17*, 353−365.
(16) Sava, G.; Gagliardi, R.; Bergamo, A.; Alessio, E.; Mestroni, G. *Anticancer Res.* **1999**, *19*, 969−972.

10.1021/ic034605i CCC: $25.00
Published on Web 08/26/2003

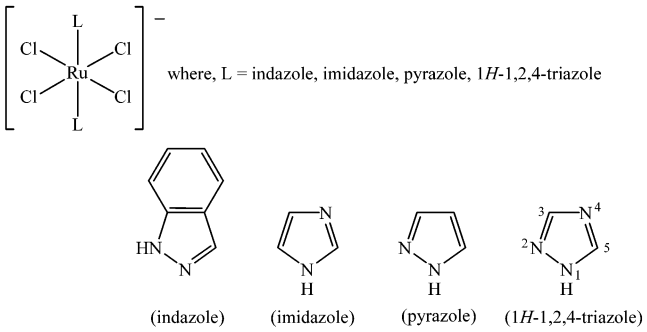

Figure 1. (Azole)Ru(III) complexes.

exhibits strong antiproliferative activity in autochtonous colorectal carcinoma in rats.[18] Remarkably, this complex showed high antitumor activity in human colon carcinoma cell lines (SW707 and SW948) in vitro comparable to that of (Hind)[*trans*-$RuCl_4(ind)_2$] (KP1019).[19] On the contrary, a related derivative, (Hpz)[*trans*-$RuCl_4(pz)_2$] (pz = pyrazole), showed only marginal activity against those cell lines, giving, however, an explicit indication on the effect of the nature of the heterocycle on biological activity.

Searching for other potent antineoplastic agents structurally related to (Hind)[*trans*-$RuCl_4(ind)_2$] and its imidazole derivative, we suggested the use of 1*H*-1,2,4-triazole (Htrz) as a heterocyclic ligand. The 2-position of the triazole is of the "pyrazole" type, while the 4-position is of the "imidazole" type (Figure 1). Looking for structure−activity relationships to be elucidated in this class of (azole)Ru(III) complexes of the type $[RuCl_4L_2]^-$, where L = azole heterocycle, we intended to study the effect of aza substitution on the imidazole or pyrazole ring, on the tumor-inhibiting activity in vitro, which could further help to create other Ru-based effective metal-based drugs. We also (i) anticipated the isolation of the *cis*/*trans* isomeric pair of $[RuCl_4(Htrz)_2]^-$ and the study of antitumor activity of both isomers (previously [*cis*-$RuCl_4L_2]^-$, L = ind, im, pz, were neither isolated nor, consequently, tested for their biological activity), and (ii) expected that increased hydrophilicity of the triazole might result in better aqueous solubility of the final complexes in comparison with rather poorly soluble (Hind)-[*trans*-$RuCl_4(ind)_2$], and that the increased solubility might facilitate the galenic formulation for eventual clinical studies. In addition, as will be discussed, the 1*H*-1,2,4-triazole exists in different tautomeric forms, and it might adopt in metal complexes both various ligating modes and those tautomeric forms which are disfavored for the free heterocycle.[20] The latter makes the coordination chemistry of this ligand toward ruthenium intriguing from the viewpoint of ligand reactivity.[21]

Herein we report on the synthesis, structure, unusual binding mode of the heterocyclic ligand, and spectroscopic properties of (triazole)Ru(III) complexes containing isomeric [*cis*-$RuCl_4(Htrz)_2]^-$ and [*trans*-$RuCl_4(Htrz)_2]^-$ anionic species. The cytotoxic activity of the two complexes (H_2trz)-[*cis*-$RuCl_4(Htrz)_2]\cdot H_2O$ (**1**) and (H_2trz)[*trans*-$RuCl_4(Htrz)_2$] (**2**) with isomeric structures assayed in vitro in three human cell lines HT29 (colon carcinoma), SK-BR-3 (breast carcinoma), and SW480 (colon carcinoma) showed (i) a clear indication for structure−activity relationship, where the *trans* complex is more active than the *cis* one, and (ii) that the activity against SW480 cell line is higher than that of (Him)-[*trans*-$RuCl_4(im)_2$].

Experimental Section

Hydrated $RuCl_3$ was purchased from Degussa and 1*H*-1,2,4-triazole from Aldrich and used as received.

Synthesis of Complexes. A starting solution of "$RuCl_3$" was prepared following the procedure described by Kralik et al.[22] Hydrated $RuCl_3$ (5.00 g; 17.7 mmol) was dissolved in a mixture of ethanol (96%)/1M HCl (250 mL, 1:1, v/v) and filtered off from an insoluble material, and the filter paper was washed with additional 5-mL portions of ethanol. The solution was refluxed on stirring for 1.5 h, allowed to cool to room temperature, then evaporated at 50 °C under reduced pressure to 38 mL, and diluted with 1 M HCl to obtain 63 mL of the dark-red "ruthenium(III) chloride" solution.

(H_2trz)[*cis*-$RuCl_4(N^2$-Htrz)$_2]\cdot H_2O$ (1) and (H_2trz)[*trans*-$RuCl_4(N^2$-Htrz)$_2$] (2). The dark-red solution of $RuCl_3$ (10.0 mL, 2.8 mmol) was added to 1*H*-1,2,4-triazole (2.00 g, 29.0 mmol). After 0.7 h, orange needles of (H_2trz)[*trans*-$RuCl_4(Htrz)_2$] (**2**) started to form, and they were filtered off after 2.5 h. For the preparation of **1**, the reaction system was left for 7 days, whereupon the precipitated mixture of large red-brown crystals of the *cis* product (**1**), orange needles of the *trans* product (**2**), and impurities were separated by filtration. The red-brown crystals of **1** were separated roughly by mechanical methods and purified by washing with five 3-mL portions of ethanol (96%) under ultrasound treatment (ca. 30 s), where all impurities and the *trans* product were dissolved. Compounds **1** and **2** were washed with two 3-mL portions of ethanol (96%) followed by two 3-mL portions of diethyl ether and dried at room temperature in air. In the case of **1**, the initial dark-red solution of $RuCl_3$ was seeded with (H_2trz)[*cis*-$RuCl_4(N^2$-Htrz)$_2]\cdot H_2O$, which was prepared with a very low yield (∼4%) by the same procedure.

(H_2trz)[*cis*-$RuCl_4(N^2$-Htrz)$_2]\cdot H_2O$ (1). Yield: 0.28 g, 21%. The complex is well soluble in water (10 mg/mL at 298 K), DMF, and DMSO, slightly soluble in methanol and ethanol, and insoluble in diethyl ether. Mp = 135−140 °C (dec). Anal. Calcd for $C_6H_{12}N_9Cl_4RuO$ (M_r = 469.10 g/mol), %: C, 15.36; H, 2.58; N, 26.87; Cl, 30.23. Found, %: C, 15.47; H, 2.56; N, 26.60; Cl, 29.88. ESI-MS (−ve), *m*/*z*: 380, $[RuCl_4(Htrz)_2]^-$; 242, $[RuCl_4]^-$. IR spectrum in KBr, selected bands, cm^{-1}: 3450 s,br; ν(OH); 3149 s; ν(CH), 626 vs; (ring torsion vibration). UV−vis (H_2O), λ_{max}, nm (ϵ, $M^{-1}\,cm^{-1}$): 405 (shoulder, 780), 358 (2420).

(H_2trz)[*trans*-$RuCl_4(N^2$-Htrz)$_2$] (2). Yield: 0.29 g, 23%. The product is soluble in water (3 mg/mL at 298 K), DMF, and DMSO, slightly soluble in methanol and ethanol, and insoluble in diethyl ether. Mp = 140 °C (dec). Anal. Calcd for $C_6H_{10}N_9Cl_4Ru$ (M_r = 451.09 g/mol), %: C, 15.97; H, 2.23; N, 27.94; Cl, 31.44. Found,

(17) Galanski, M.; Arion, V. B.; Jakupec, M. A.; Keppler, B. K. *Curr. Pharm. Des.*, submitted.
(18) Berger, M. R.; Garzon, F. T.; Keppler, B. K. *Anticancer Res.* **1989**, *9*, 761−766.
(19) Galeano, A.; Berger, M. R.; Keppler, B. K. *Arzneim-Forsch.* **1992**, *6*, 821−824.
(20) Haasnoot, J. G. *Coord. Chem. Rev.* **2000**, *200*−*202*, 131−185.
(21) Pombeiro, A. J. L.; Kukushkin, V. Yu. *Reactions of Coordinated Ligands: General Considerations* In, *Comprehensive Coordination Chemistry*, 2nd ed.; Lever, A. B. P., Ed.; Elsevier: New York; Vol. 1, in press.
(22) Kralik, F.; Vrestal, J. *Collect. Czech. Chem. Commun.* **1961**, *26*, 1298−1304.

%: C, 15.87; H, 2.43; N, 27.66; Cl, 30.89. ESI-MS (−ve): *m*/*z* 380, $[RuCl_4(Htrz)_2]^-$; 242 $[RuCl_4]^-$. IR spectrum in KBr, selected bands, cm^{-1}: 3131 s; ν(CH), 626 vs; (ring torsion vibration). UV−vis (H_2O), λ_{max}, nm (ϵ, M^{-1} cm^{-1}): 420 (370), 365 (2745), 240 (9420).

$(Ph_3PCH_2Ph)[trans\text{-}RuCl_4(N^2\text{-}Htrz)_2]\cdot H_2O$ (3). A solution of $(Ph_3PCH_2Ph)Cl$ (0.066 g, 0.17 mmol) in ethanol (3 mL) was added to a solution of $(H_2trz)[trans\text{-}RuCl_4(Htrz)_2]$ (0.075 g, 0.17 mmol) in water (25 mL). The light-orange microcrystals which immediately formed were filtered off, washed with ethanol and diethyl ether, and dried at room temperature in air. Yield: 0.09 g, 77%. The complex is soluble in DMSO, sparingly soluble in DMF and methanol, and insoluble in water and diethyl ether. Mp = 195 °C (dec). Anal. Calcd for $C_{29}H_{30}N_6RuCl_4OP$ (M_r = 752.44 g/mol), %: C, 46.29; H, 4.02; N, 11.17; Cl, 18.85. Found, %: C, 46.17; H, 4.03; N, 11.10; Cl, 18.65. ESI-MS (−ve), *m*/*z*: 380, $[RuCl_4(Htrz)_2]^-$; 242, $[RuCl_4]^-$; ESI-MS(+ve), *m*/*z*: 353, $[Ph_3PCH_2Ph]^+$. IR spectrum in KBr, selected bands, cm^{-1}: 3470 s,br; ν(OH), 3145 m; ν(CH), 625 m; (ring torsion vibration). UV−vis (MeOH), λ_{max}, nm (ϵ, M^{-1} cm^{-1}): 435 (380), 375 (3400).

Physical Measurements. Elemental analyses were carried out by the Microanalytical Service of the Instituto Superior Técnico in Lisbon or on a Carlo Erba microanalyzer at the Institute of Physical Chemistry of the University of Vienna. Infrared spectra were recorded on a Perkin-Elmer FTIR 2000 IR spectrometer in KBr pellets (4000−400 cm^{-1}). UV−vis spectra were recorded on a Perkin-Elmer Lambda 20 UV−vis spectrometer using samples dissolved in water or methanol. Electrospray ionization mass spectrometry was carried out with a Bruker Esquire 3000 instrument (Bruker Daltonic, Bremen, Germany). The given *m*/*z* values, originating from the most intense isotopes, were obtained by the mass linearization procedure. Expected and experimental isotope distributions were compared. Melting points were measured on a Kofler-table (Leica Galen III). Cyclic voltammograms were measured in a two-compartment three-electrode cell using a 0.5-mm-diameter platinum-disk working electrode or alternatively with an glassy carbon electrode (Ø=1.0 mm), probed by a Luggin capillary connected to a silver wire pseudo-reference-electrode and a platinum auxiliary electrode. Measurements were performed at room temperature using an EG&G PARC 273A potentiostat/galvanostat. Deaeration of solutions was accomplished by passing a stream of high-purity nitrogen through the solution for 10 min prior to the measurements and then maintaining a blanket atmosphere of nitrogen over the solution during the measurements. The potentials were measured in 0.2 M $[n\text{-}Bu_4N][BF_4]$/DMF, at a scan rate of 200 mV/s, and are quoted relative to the $[Fe(\eta^5\text{-}C_5H_5)_2]^{0/+}$ redox couple ($E_{1/2}{}^{ox}$ = 0.72 V vs NHE),[23] which was used as internal standard, employing a platinum disk working electrode.

Crystallographic Structure Determination. X-ray diffraction measurements were performed on a Nonius Kappa CCD diffractometer at 120 K. Single crystals were positioned at 35 and 30 mm from the detector, and 676 and 341 frames were measured, each for 10 and 120 s over a 1.5° and 2° scan for **1** and **3** correspondingly. The data were processed using Denzo-SMN software. Crystal data, data collection parameters, and structure refinement details for **1** and **3** are given in Table 1. The structures were solved by direct methods and refined by full-matrix least-squares techniques. Non-hydrogen atoms were refined with anisotropic displacement parameters. H atoms were located on difference Fourier maps and isotropically refined. The following computer programs were used: structure solution, SHELXS-97,[24] refinement, SHELXL-97,[25] molecular diagrams, ORTEP,[26] computer, Pentium II; scattering factors.[27]

Table 1. Crystal Data and Details of Data Collection for **1** and **3**

	1	**3**
empirical formula	$C_6H_{12}N_9Cl_4ORu$	$C_{29}H_{30}N_6Cl_4OPRu$
fw	469.12	752.43
space group	$P2_1/c$	$P2_1/c$
a, Å	9.474(2)	11.605(2)
b, Å	8.794(2)	17.149(3)
c, Å	18.343(4)	16.023(3)
β, deg	94.40(3)	97.81(3)
V, Å^3	1523.7(6)	3159.2(10)
Z	4	4
λ, Å	0.71073	0.71073
ρ_{calcd}, g cm^{-3}	2.045	1.582
cryst size, mm^3	0.14 × 0.26 × 0.31	0.015 × 0.22 × 0.35
T, K	120	120
μ, cm^{-1}	17.42	9.20
R1[a]	0.0225	0.0268
wR2[b]	0.0568	0−0621
GOF[c]	1.027	1.029

[a] $R1 = \sum||F_o| - |F_c||/\sum|F_o|$. [b] $wR2 = \{\sum[w(F_o^2 - F_c^2)^2]/\sum[w(F_o^2)^2]\}^{1/2}$. [c] $GOF = \{\sum[w(F_o^2 - F_c^2)^2]/(n-p)\}^{1/2}$, where *n* is the number of reflections and *p* is the total number of parameters refined.

Cell Lines and Culture Conditions. Three human cell lines were used for cytotoxicity experiments as described: HT29 and SW480 (adenocarcinoma of the colon) were kindly provided by Brigitte Marian (Institute of Cancer Research, University of Vienna, Austria), and SK-BR-3 (adenocarcinoma of the breast) was a gift from Evelyn Dittrich (General Hospital, University of Vienna, Austria). Cells were grown as adherent monolayer cultures in minimum essential medium (MEM) containing 10% heat-inactivated fetal bovine serum, 2 mM L-glutamine, 1 mM sodium pyruvate, 50 μg/mL streptomycin, and 50 U/mL penicillin (all purchased from Gibco). Cultures were maintained at 37 °C in a humidified atmosphere containing 5% CO_2.

Drug Cytotoxicity. Monolayer cell cultures were trypsinized, and single-cell suspensions were obtained by repeated pipetting. A final cell density of 3×10^4, 1.5×10^4 and 3×10^4 cells/mL for HT29, SW480 and SK-BR-3, correspondingly, was prepared in complete culture medium, and 200 μL cell suspension was added to each well of a 96-well microculture plate. On the day following plating, medium was removed, and compounds were added at the respective concentrations dissolved in complete culture medium. Each concentration was given to eight microcultures in parallel.

The MTT assay was performed after the cells had been incubated for 24 and 96 h. Cells treated for 24 h were incubated in drug-free culture medium for a further 72 h before the MTT dye was added whereas the MTT reaction was performed immediately after drug exposure in the case of the 96 h treatment. 3-(4,5-Dimethylthiazol-2-yl)-2,5-diphenyltetrazoliumbromide (MTT) was dissolved in aqua tridest at 5 mg/mL, and 20 μL was added to each well already filled with a fresh 150 μL portion of complete culture medium and incubated for 4 h at 37 °C. Afterward, the precipitated dye was dissolved in 150 μL DMSO, and optical densities were measured at a wavelength of 550 nm by means of a microplate reader (Tecan Spectra Classic). Each experiment was performed in triplicate, and evaluation is based on means.

(23) Barrette, W. C., Jr.; Johnson, H. W., Jr.; Sawyer, D. T. *Anal. Chem.* **1984**, *56*, 1893−1898.

(24) Sheldrick, G. M. *SHELXS-97, Program for Crystal Structure Solution*; University Göttingen: Göttingen, Germany, 1997.

(25) Sheldrick, G. M. *SHELXL-97, Program for Crystal Structure Refinement*; University Göttingen: Göttingen, Germany, 1997.

(26) Johnson, C. K. Report ORNL-5138; Oak Ridge National Laboratory: Oak Ridge, TN, 1976.

(27) *International Tables for X-ray Crystallography*; Kluwer Academic Press: Dordrecht, The Netherlands, 1992; Vol. C, Tables 4.2.6.8 and 6.1.1.4.

Scheme 1

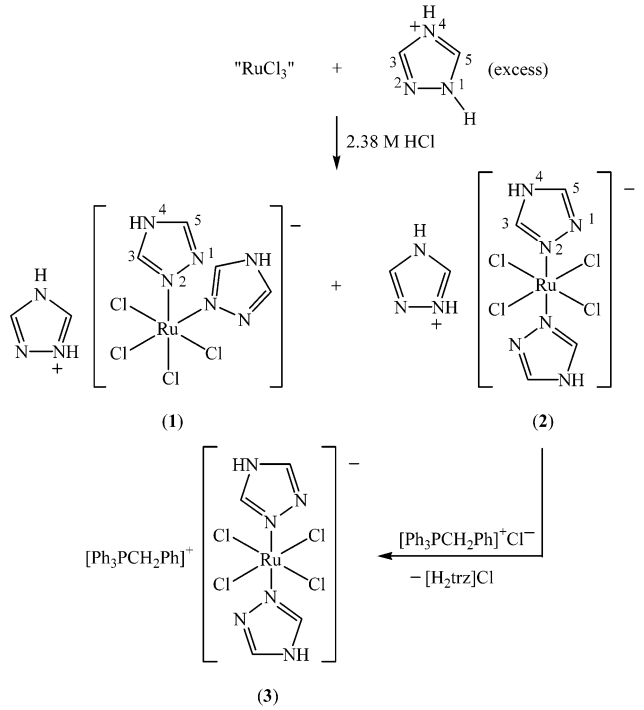

Results and Discussion

Synthesis and Characterization of Complexes. Ruthenium(III) chloride reacts with an excess of 1*H*-1,2,4-triazole in 2.38 M HCl solution (where the heterocycle exists as the triazolium salt; $pK_a = 2.55$[28]) to give two products isolated as the solid $(H_2trz)[cis\text{-}Ru^{III}Cl_4(Htrz)_2]\cdot H_2O$ (**1**) as large red-brown blocks and $(H_2trz)[trans\text{-}Ru^{III}Cl_4(Htrz)_2]$ (**2**) as orange needles (Scheme 1). While the crystals of **1** proved to be suitable for an X-ray structure determination, our attempts to prepare single crystals of **2** for an X-ray data set collection resulted in crystals of rather poor quality, which however permitted us to establish the *trans* arrangement of the two triazole ligands in the complex anion. In addition, a metathesis reaction between **2** and triphenylbenzylphosphonium chloride has been carried out to obtain **3** (Scheme 1), which was studied by X-ray crystallography (see following description). Complexes **1** and **2** show, as expected, better water solubility than the indazole derivative (Hind)[*trans*-$RuCl_4(ind)_2$]. Aqueous solubility is often the major problem precluding the clinical use of potent metal-based drugs. Note also that the solubility of **1** is significantly higher than that of **2** (see Experimental Section). The negative ion ESI mass spectra of **1**−**3** showed a 100% intense peak at *m*/*z* 380 due to $[Ru^{III}Cl_4(Htrz)_2]^-$ ions. Their isotopic patterns in the mass spectra agree well with the calculated isotopic distribution. Another peak observed in all three cases was detected at *m*/*z* 242 and corresponds to the $[Ru^{III}Cl_4]^-$ ion. The positive ion mass spectrum of **3** displayed a peak at *m*/*z* 353 arising from the $Ph_3PCH_2Ph^+$ cation.

The electronic absorption spectrum of **1** in water shows one band with an absorption maximum at 358 nm ($\epsilon = 2420$ M^{-1} cm^{-1}) and a shoulder at ~405 nm ($\epsilon = 780$ M^{-1} cm^{-1}) and differs, as expected, from that of **2**, in which three bands at 240 nm ($\epsilon = 9425$ $M^{-1}cm^{-1}$), 365 nm ($\epsilon = 2745$ $M^{-1}cm^{-1}$), and 420 nm ($\epsilon = 370$ M^{-1} cm^{-1}) are observed. The latter two bands are red-shifted in methanol solution of **3** to 375 nm ($\epsilon = 3400$ M^{-1} cm^{-1}) and 435 nm ($\epsilon = 380$ M^{-1} cm^{-1}), which can presumably be assigned to chloride $p\pi \rightarrow$ Ru $d\pi$ LMCT transitions.[29]

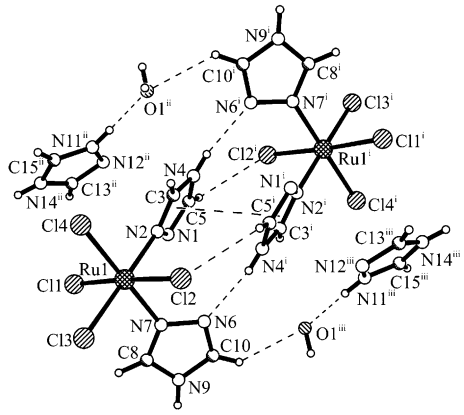

Figure 2. Part of the crystal structure of **1** showing the formation of a stack pair by $\pi-\pi$ interaction between two adjacent triazole ligands. Atoms marked with i, ii, and iii are at the symmetry positions $(-x + 1, -y + 1, -z + 1)$, $(x - 1, y, z)$, and $(-x + 2, -y + 1, -z + 1)$, respectively.

Table 2. Bond Lengths (Å) and Angles (deg) in the Coordination Polyhedron and in the Coordinated Triazole Ligands of **1** and **3**

atom1−atom2	**1**	**3A**	**3B**
Ru1−N2	2.0627(10)	2.0668(13)	
Ru1−N7	2.0733(10)		
Ru2−N7			2.0575(14)
Ru1−Cl1	2.3663(6)	2.3493(6)	
Ru1−Cl2	2.3628(6)	2.3591(6)	
Ru1−Cl3	2.3870(5)		
Ru1−Cl4	2.3478(5)		
Ru2−Cl3			2.3557(7)
Ru2−Cl4			2.3671(9)
N1−N2	1.3775(13)	1.3734(18)	
N2−C3	1.3205(15)	1.3146(19)	
C3−N4	1.3483(15)	1.340(2)	
N4−C5	1.3554(15)	1.341(2)	
C5−N1	1.3127(15)	1.312(2)	
N6−N7	1.3868(14)		1.3783(18)
N7−C8	1.3127(15)		1.313(2)
C8−N9	1.3461(15)		1.341(2)
N9−C10	1.3516(17)		1.343(2)
C10−N6	1.3164(16)		1.316(2)
atom1−atom2−atom3	**1**	**3A**	**3B**
N1−N2−C3	108.21(9)	107.48(12)	
N2−C3−N4	109.14(10)	109.70(14)	
C3−N4−C5	105.85(10)	105.90(13)	
N4−C5−N1	110.57(10)	110.46(14)	
C5−N1−N2	106.24(9)	106.46(13)	
N6−N7−C8	108.63(9)		107.81(13)
N7−C8−N9	109.23(10)		109.95(14)
C8−N9−C10	105.85(10)		105.43(14)
N9−C10−N6	111.05(11)		111.11(15)
C10−N6−N7	105.23(10)		105.69(13)

Crystal Structures. The asymmetric unit of **1** contains an essentially octahedral anion $[RuCl_4(Htrz)_2]^-$, the triazolium cation, and a water molecule. A part of the crystal structure of **1** is shown in Figure 2. Selected bond distances and angles are quoted in Table 2.

(28) Potts, K. T. *Chem. Rev.* **1961**, *61*, 87−127.

(29) Rack, J. J.; Gray, H. B. *Inorg. Chem.* **1999**, *38*, 2−3.

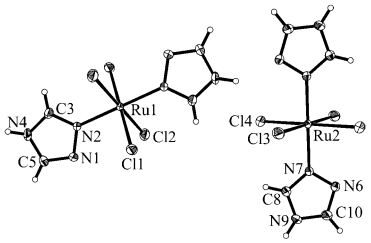

Figure 3. View of two independent complex anions of **3** (**A** and **B**), showing the atom-labeling scheme. Displacement ellipsoids are drawn at the 50% probability level.

The ruthenium(III) atom is bound to two, *cis* arranged to each other, monodentate triazole ligands and four chloride anions. The Ru−N2 and Ru−N7 bond distances at 2.0627(10) and 2.0733(10) Å, respectively, are comparable with those in (Ph_4P)[*trans*-$RuCl_4(ind)_2$] at 2.0517(21) and 2.0711(22) Å.[30] The triazole ligands coordinated via N2 and N7 are tilted relative to the mean plane through RuN2N7Cl3Cl4, the corresponding angles being at 42.5° and 138.7°. The Ru−Cl bond distances (Table 2) are normal for ruthenium(III) complexes.[31−33] The most striking feature, however, is the stabilization of the 4*H* tautomeric form of the 1,2,4-triazole in this species through binding of the ligand via N2 to ruthenium(III) ion. To the best of our knowledge, no such behavior has been observed for any other metal ions so far, and this gives a novel example for predominant stabilization by complexation of a tautomer which is the minor one in the metal-free ligands.[21]

It is worth mentioning the formation of stacked pairs of $[RuCl_4(Htrz)_2]^-$ through $\pi-\pi$ intermolecular interaction between triazole planes as shown in Figure 2. For the triazole rings of adjacent anions, the minimum distance between the ring centroids of the interacting species is ca. 3.38 Å, with the planes separated by 3.10 Å. In addition, the built dimeric species is stabilized by strong H-bonding interactions. All nitrogen atoms of the coordinated triazole ligands are involved in hydrogen bonding. The hydrogen atoms of the water molecule appear to take part in two bifurcated hydrogen bonds, involving Cl2 and Cl3. Other intermolecular contacts involving the triazolium cation and water molecule are shown in Figure 2.

The asymmetric unit of **3** contains two crystallographically distinct $RuCl_2(Htrz)$ moieties, each of them being a half of the *trans*-$[RuCl_4(Htrz)_2]^-$, with Ru1 and Ru2 situated on crystallographic inversion points, a $Ph_3PCH_2Ph^+$ cation and a water molecule. Both Ru1 and Ru2 are coordinated by a pair of symmetry related *trans*-triazole ligands and four symmetry related chloride ions in an octahedral manner. The structures of the complex anions **3A** and **3B** are shown in Figure 3. Selected bond distances and angles are given in Tables 2 and 3. The Ru1−N2 and Ru2−N7 at 2.0668(13) and 2.0575(14) Å compare well with those in *cis* species **1**. The *trans*-arranged triazole ligands are almost parallel to each other and bisect the angles Cl1−Ru1−Cl2 and Cl3−Ru2−Cl4 in **3A** and **3B**, correspondingly. The torsion angles N1−N2···N2A−C3A and N6−N7···N7A−C8A are at 3.3° and −0.8° in **3A** and **3B**, respectively. Like in **1**, the triazole ligands adopt the 4*H* tautomeric form, being coordinated through N2 in the nomenclature used for 1*H*- or 4*H*-1,2,4-triazole. The Ru−Cl bond distances vary from 2.3493(6) to 2.36.71(9) Å and do not present unexpected features.

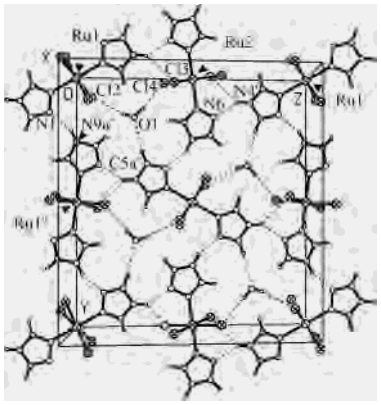

Figure 4. Part of the crystal structure of **3** showing the formation of a (100) sheet built from complex anions and water molecules. Atoms marked i and ii are at the symmetry positions (x, y, $z + 1$) and ($-x$, $0.5 + y$, $0.5 - z$), respectively.

Table 3. Bond Lengths (Å) and Angles (deg) in the Triazolium Cation in **1**

atom1−atom2	**1**
N11−N12	1.3644(16)
N12−C13	1.3070(18)
C13−N14	1.3556(18)
N14−C15	1.3295(17)
C15−N11	1.3116(16)
atom1−atom2−atom3	**1**
N11−N12−C13	103.69(11)
N12−C13−N14	111.44(12)
C13−N14−C15	106.37(11)
N14−C15−N11	107.24(12)
C15−N11−N12	111.25(11)

The packing diagram reveals a layered structure composed of alternating sheets of hydrogen bonded anionic $[RuCl_4(Htrz)_2]^-$ species, water molecules (Figure 4), and $Ph_3PCH_2Ph^+$ cations. Between sheets there are weak interactions of the C−H···Cl type.

Although the structures of both isomeric species have been unequivocally established by X-ray crystallography, the mode of coordination of 1,2,4-triazole in them deserves some additional comments which are given in the following paragraphs.

Coordination Mode of Triazole. The coordination chemistry of 1,2,4-triazole shows interesting features,[20] mainly because of the diverse modes of binding to metal ions and tautomerism. There are known two NH-tautomeric forms 1*H* and 4*H* for 1,2,4-triazole, which differ from each other in electron distribution and in the position of a relatively acidic NH group.

(30) Peti, W.; Pieper, T.; Sommer, M.; Keppler, B. K.; Giester, G. *Eur. J. Inorg. Chem.* **1999**, 1551−1555.
(31) Alessio, E.; Balducci, G.; Lutman, A.; Mestroni, G.; Calligaris, G.; Attia, W. M. *Inorg. Chim. Acta* **1993**, *203*, 205−217.
(32) Jasval, J. S.; Rettig, S. J.; James, B. R. *Can. J. Chem.* **1990**, *68*, 1808−1817.
(33) Alessio, E.; Balducci, G.; Calligaris, M.; Costa, G.; Attia, W. M.; Mestroni, J. *Inorg. Chem.* **1991**, *30*, 609−618.

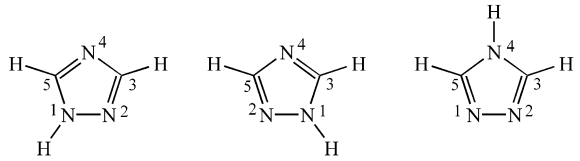

1*H* (**A**) 1*H* (**B**) 4*H* (**C**)

Figure 5. Tautomeric forms of 1,2,4-triazole.

The species 1*H*(**A**) and 1*H*(**B**) are statistically distinct, but energetically equal (Figure 5).[34] Therefore, it implies that the 1*H* tautomer is twice as probable as 4*H*. Dipole moment measurements of 1,2,4-triazole in dioxane indicated the presence of some amount of 4*H*-tautomer in solution.[35] Analogously, ^{15}N NMR studies showed the presence of about 40% of 4*H*-tautomer in concentrated solutions of Htrz in methanol.[36] In the solid, Htrz crystallizes exclusively as a 1*H*-tautomer.[37−39] However, the 4*H*-tautomer can be stabilized upon ligation to metal centers. In addition, 1,2,4-triazole can act in metal complexes as a neutral ligand or as a triazolate anion $(trz)^-$. Moreover, the 1*H*-1,2,4-triazole can easily be derivatized. More than 200 X-ray diffraction structures are well documented,[20] of them only 10% concern the metal complexes of the unsubstituted 1,2,4-triazole. This behaves as monodentate ligand coordinating to the first row or second row transition metal ion through N4 ($[Mn^{II}(SO_4)(Htrz)(H_2O)_4]$,[40] $[Cd(NCS)_2(Htrz)_2]$,[41] $[FeCl_3(bpy)(Htrz)]$,[42] or Zn(II) in human carbonic anhydrase[43]) when neutral or via N1 ($[Au(trz)(PPh_3)]_2$,[44] $[PhC(CH_3)_2CH_2]_3Sn(trz)$[45]) when deprotonated. *exo*-Didentate linking of metal ions through two nonadjacent nitrogens is a feature of both triazole and triazolate ligands. The *exo*-didentate N2, N4 binding mode was found in a number of compounds with general formulas $[M^{II}(NCS)_2(Htrz)_2]$, where M = Fe,[46] Co,[47,48] Mn,[49] Zn, and Cu.[47] *exo*-Didentate N1, N4 linking of triazolate anion has been discovered in *trans*-$\{[(NH_2Me)_2Pt^{II}(mecyt)_2Pd^{II}]_2(trz)\}(NO_3)_3$ (mecyt = 1-methylcytosinato)[50] and in a helical polymer complex $[Ag^{I}(trz)(PPh_3)_2]_n$.[51] The 4*H* tautomer stabilization occurs probably when the N1, N2 *endo*-bridging mode is adopted, as in $[CuCl_2(Htrz)]$,[52] $[CuBr_2(Htrz)]$,[53] $[Ni_3(Htrz)_6(H_2O)_6](NO_3)_6$,[54,55] $[MoO_3(Htrz)_{0.5}]_n$,[56] $[Rh^{I}_3(\mu\text{-Htrz})(\eta^3\text{-}C_3H_5)_6]$,[57] or $[Ag(NO_3)(Htrz)]_2$.[58] The triply bridging triazolato group has been documented for ZnCl(trz),[59] $[\{Cu_3(trz)_2\}V_4O_{12}]_n$,[60] and two rhodium(I) complexes $[Rh_3(\mu_3\text{-trz})(\mu\text{-Cl})Cl(\eta^4\text{-tfbb})(CO)_4]\cdot 0.5CH_2Cl_2$ (tfbb = tetrafluorobenzobarrelene)[61] and $[Rh_3(\mu\text{-Cl})Cl(\mu_3\text{-trz})(\eta^3\text{-}C_3H_5)_2(CO)_4]\cdot 0.5C_2H_4Cl_2$.[57]

In both isomers, the coordination of 1,2,4-triazole to ruthenium via N2 has been found. These are the first known complexes in which triazole acts as a monodentate ligand being bound via N2 to a metal ion. The N2 atom in triazole is less basic than N4;[62] therefore, such a behavior is rather unexpected. The reason is probably the acidic reaction medium, which is needed to avoid the deprotonation of the 1*H*-1,2,4-triazole upon coordination. Moreover, we suggest that N4 is easily protonated under these conditions and N2 possessing a lone pair is probably imposed to coordinate to ruthenium with subsequent rearrangement of the azole ring double bonds and deprotonation at N1, due to the polarization effect of Ru^{3+}, which is more close to the positively charged metal center than N4.

Cyclic Voltammetric Studies. The cyclic voltammograms of **1** [Figure 6 (top)], **2**, and **3** [Figure 6 (bottom)] in DMF, at a platinum disk working electrode, at the scan rate 200 mV/s, display one single-electron oxidation wave (I^{ox}) that meets the usual reversibility and diffusion controlled electron-transfer criteria, at $E_{1/2}^{ox}$ = 0.33, 0.46, and 0.45 V versus FcH/FcH^+, respectively, assigned to the Ru(III) to Ru(IV) oxidation, and one irreversible reduction wave (I^{red}) at E_p^{red} = −1.23, −1.24, and −1.26 V, correspondingly, due to the Ru(III) to Ru(II) reduction. Another irreversible reduction wave is observed at E_p^{red} = −0.92 V in **1** and **2**, but it disappears in **3**, or when a glassy carbon working electrode is used in **1** or **2**, and is associated to the reduction of the protic counterion H_2trz^+. Irreversible oxidation waves at E_p^{ox} = −0.82, −0.63, and 0.66 V in **1**, −0.88, −0.64, and 0.67

(34) Claramunt, R. M.; López, C.; Garcia, M. A.; Otero, M. D.; Torres, M. R.; Pinilla, E.; Alarcón, S. H.; Alkorta, I.; Elguero, J. *New J. Chem.* **2001**, *25*, 1061−1068.
(35) Mazheika, I. B.; Chipen, G. I.; Hiller, S. A. *Khim. Geterotsikl. Soedin.* **1966**, 776−781.
(36) Witanowski, M.; Stefaniak, L.; Januszewski, H.; Grabowski, Z.; Webb, G. A. *Tetrahedron* **1972**, *28*, 637−653.
(37) Goldstein, P.; Ladell, J.; Abowitz, G. *Acta Crystallogr.* **1969**, *B25*, 135−143.
(38) Jeffrey, G. A.; Ruble, J. R.; Yates, J. H. *Acta Crystallogr.* **1983**, *B39*, 388−394.
(39) Fuhrmann, P.; Koritsanszky, T.; Luger, P. *Z. Kristallogr.* **1997**, *212*, 213−220.
(40) Schomburg, D.; Link, M.; Linoh, H.; Tacke, R. *J. Organomet. Chem.* **1988**, *339*, 69−80.
(41) Corter, S.; Engelfriet, D. W. *Acta Crystallogr.* **1981**, *B37*, 1214−1218.
(42) Haasnoot, J. G.; De Keyzer, G. C. M.; Verschoor, G. C. *Acta Crystallogr.* **1983**, *C39*, 1207−1209.
(43) Driessen, W. L.; De Graaf, R. A. G.; Vos, J. G. *Acta Crystallogr.* **1983**, *C39*, 1635−1637.
(44) Mangani, S.; Liljas, A. *J. Mol. Biol.* **1993**, *232*, 9−14.
(45) Nomiya, K.; Noguchi, R.; Ohsawa, K.; Tsuda, K. *J. Chem. Soc., Dalton Trans.* **1998**, 4101−4108.
(46) Engelfriet, D. W.; Verschoor, G. C. *Acta Crystallogr.* **1981**, *B37*, 237−240.
(47) Engelfriet, D. W.; Den Brinker, W.; Verschoor, G. C.; Gorter, S. *Acta Crystallogr.* **1979**, *B35*, 2922−2927.
(48) Engelfriet, D. W.; Groeneveld, W. L.; Groenendijk, H. A.; Smit, J. J.; Nap, G. M. *Z. Naturforsch.* **1980**, *35a*, 115−128.
(49) Engelfriet, D. W.; Groeneveld, W. L.; Nap, G. M. *Z. Naturforsch.* **1980**, *35a*, 1387−1389.
(50) Pichierri, F.; Chiarparin, E.; Zangrando, E.; Randaccio, L.; Holthenrich, D.; Lippert, B. *Inorg. Chim. Acta* **1997**, *264*, 109−116.
(51) Nomiya, K.; Tsuda, K.; Kasuga, N. C. *J. Chem. Soc., Dalton Trans.* **1998**, 1653−1659.
(52) Jarvis, J. A. J. *Acta Crystallogr.* **1962**, *15*, 964−966.
(53) Asaji, T.; Sakai, H.; Nakamura, D. *Inorg. Chem.* **1983**, *22*, 202−206.
(54) Reimann, C. W.; Zocci, M. *J. Chem. Soc., Chem. Commun.* **1968**, 272.
(55) Reimann, C. W.; Zocci, M. *Acta Crystallogr.* **1971**, *B27*, 682−691.
(56) Hagrman, P. J.; LaDuca, R. L., Jr.; Koo, H.-J.; Rarig, R., Jr.; Haushalter, R. C.; Whangbo, M.-H.; Zubieta, J. *Inorg. Chem.* **2000**, *39*, 4311−4317.
(57) Oro, L. A.; Pinillos, M. T.; Tejel, C.; Foces-Foces, C.; Cano, F. H. *J. Chem. Soc., Dalton Trans.* **1986**, 2193−2200.
(58) Schmidbaur, M.; Mair, A.; Müller, G.; Lachmann, J.; Gamper, S. *Z. Naturforsch.* **1991**, *46b*, 912−918.
(59) Kröber, J.; Bkouche-Waksman, I.; Pascard, C.; Thomann, M.; Kahn, O. *Inorg. Chim. Acta* **1995**, *230*, 159−163.
(60) Hagrman, P. J.; Bridges, C.; Greedan, J. E.; Zubieta, J. *J. Chem. Soc., Dalton Trans.* **1999**, 2901−2903.
(61) Oro, L. A.; Pinillos, M. T.; Tejel, C.; Foces-Foces, C.; Cano, F. H. *J. Chem. Soc., Dalton Trans.* **1986**, 1087−1094.
(62) Meot-Ner, M.; Liebman, J. F.; Del Bene, J. E. *J. Org. Chem.* **1986**, *51*, 1105−1110.

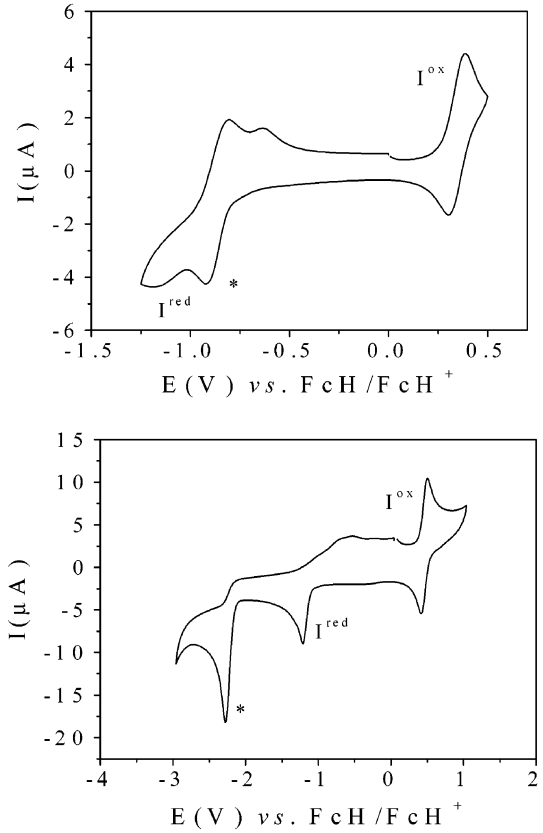

Figure 6. Cyclic voltammogram of **1** in DMF at scan rate 200 mV/s with a platinum working electrode (top) and of **3** in DMF at scan rate 200 mV/s with a glassy carbon working electrode (bottom). Asterisk indicates reduction wave of the H_2trz^+ counterion.

V in **2**, and −0.86, −0.66, and 0.64 V in **3** are detected upon scan reversal following the cathodic scan.

The current function ($i_p v^{-1/2} c^{-1}$, where i_p is the peak current, v is the scan rate, and c is the concentration) of the oxidation wave at −0.82 in **1**, −0.88 in **2**, or −0.86 V in **3**, which is maximum at higher scan rates, decreases with the decrease of the scan rate with concomitant increase of the current function of the oxidation wave at − 0.63 in **1**, − 0.64 in **2**, or −0.66 V in **3**. This indicates the cathodic formation of an intermediate (oxidized at the former wave) that is further converted into the thermodynamic product oxidized at the latter wave, which is better seen at lower scan rates (Figures S1−S4).

The oxidation wave at 0.66 in **1**, 0.63 in **2**, or 0.64 V in **3** can be assigned to the oxidation of chloride, liberated upon cathodic reduction of the complexes as known[63] to occur on chemical reduction of Ru(III)−chloro complexes. This is also consistent with reported observations[64] for this type of complexes and is further supported by the fact that addition of $[Ph_3PCH_2Ph]Cl$ to the solution revealed chloride oxidation at ca. 0.65 V. Comparison of the oxidation potentials of the various complexes indicates that the *cis* isomer (in **1**) is easier to oxidize than the *trans* one (in **2** and **3**), indicating a more stabilized HOMO in the latter isomer.

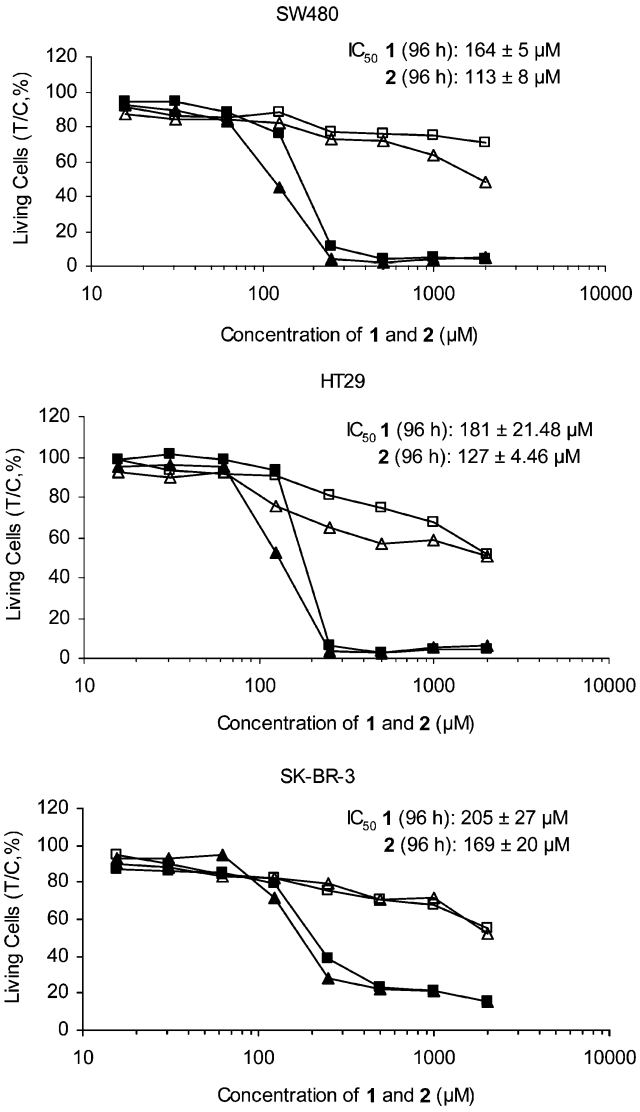

Figure 7. Dose−response curves of the complexes **1** (■ 96 h, □ 24 h), and **2** (● 96 h; ○ 24 h) in colon carcinoma cells SW480 (top) and HT29 (middle) and in mammary carcinoma cells SK-BR-3 (bottom) after 24 h and 96 h of exposure under standard conditions (pH 7.4). Each data point is the mean of three independent determinations.

Lever's redox potential parametrization approach[65] for octahedral complexes of reversible Ru^{III}/Ru^{II} couples assuming ligand additivity allows us to estimate the redox potentials for our complexes. The thus calculated potential, $E_{1/2}^{red} = -1.26$ V (estimated by considering the E_L value of 0.18 V versus NHE for the 1,2,4-triazole ligand, in complexes studies in organic solvents), is in very good agreement with the measured reduction potentials (see preceding details), although the latter correspond to irreversible waves and to the unusual N2-coordination mode of 1,2,4-triazole. However, one should mention that this agreement in organic solvents cannot be extrapolated to aqueous medium, where the Ru^{III}/Ru^{II} redox potentials shift anodically and are pH dependent as already demonstrated for (Him)[*trans*-$RuCl_4(im)_2$].[66] Further investigation of our systems in aqueous media is under way.

(63) Ford, P. C. *Coord. Chem. Rev.* **1970**, *5*, 75−99.
(64) Serli, B.; Zangrando, E.; Iengo, E.; Mestroni, G.; Yellowlees, L.; Alessio, E. *Inorg. Chem.* **2002**, *41*, 4033−4043.
(65) Lever, A. B. P. *Inorg. Chem.* **1990**, *29*, 1271−1285.
(66) Ni Dhubhghaill, O. M.; Hagen, W. R.; Keppler, B. K.; Lipponer, K. G.; Sadler, P. J. *J. Chem. Soc., Dalton Trans.* **1994**, 3305−3310.

Cytotoxicity in Human Carcinoma Cell Lines. Responses of SW480, HT29 (colon carcinoma), and SK-BR-3 (mammary carcinoma) cells to continuous exposure to various concentrations of **1** and **2** for 24 and 96 h are presented in Figure 7. Two remarkable features become evident: (i) Time-dependent response of all three cell lines to **1** and **2** has been observed. No marked antiproliferative effect is seen after 24 h of drug-exposure time in concentrations up to 2000 μM; in neither case was the IC_{50} reached. In contrast, the effect is evident after 96 h. This can be due to slow activating reactions of the complexes in the medium or slow incorporation mode into the cell. Which of these mechanisms is responsible for this observation has to be determined by further experiments. The fact that the marked time dependence of the cell damage is observed despite extended postincubation after the 24-h treatment indicates that intracellular activation of the compounds cannot explain this effect. (ii) The structure−activity relationship is worth mentioning. The *trans* isomer, **2**, shows higher antiproliferative activity in all three human carcinoma cell lines, as compared to *cis* compound **1**, the difference being more pronounced on colon carcinoma cells than on the mammary cell line.

The *trans* complex, **2**, shows even higher antiproliferative activity after the 96 h treatment on SW480 than (Him)[*trans*-$RuCl_4(im)_2$] (IC_{50} = 840 μM for imidazole complex;[67] 113 ± 8 μM for **2**), leading to further interest in comparing *trans* and *cis* complexes to figure out whether the ligand or the configuration of the complex is more important for evolving activity.

Final Remarks. For the first time, both *trans* and *cis* isomers of (azole)Ru(III) complexes of the type $[RuCl_4L_2]^-$, where L = azole heterocycle, have been prepared, in which unprecedented monodentate coordination of triazole via N2 and stabilization of the 4*H* tautomeric form have been observed. This work demonstrates the availability of both isomers for complexes of the type $[RuCl_4L_2]^-$ and makes the search for *cis* isomers with species other than triazole heterocycles relevant. The performed preparative studies gave a unique opportunity to carry out structure−activity relationships for such type of complexes. Compounds **1** and **2** show considerable in vitro antitumor activity in three human cell lines: SW480, HT29, and SK-BR-3, the activity against SW480 being higher than for (Him)[*trans*-$RuCl_4(im)_2$]. It is worth mentioning that in contrast to $PtCl_2(NH_3)_2$, where the *trans*-species exhibits only marginal tumor-inhibiting activity, the activity of *trans* product **2** was superior to that of *cis* complex **1**, suggesting another mechanism of action than that for cisplatin. As expected, both isomeric species are significantly more water-soluble than the indazole derivative (Hind)[*trans*-$RuCl_4(ind)_2$], which suggest them as compounds of great potential for development as anticancer drugs. Studies on their anticancer activity in vivo, hydrolytic stability, interaction with biologically relevant targets, and cell uptake of Ru species are under way in our group.

Acknowledgment. The authors are indebted to FWF, COST, the Foundation for Science and Technology and the POCTI-programme (Portugal) for financial support. We also thank Dr. G. Giester for X-ray data collection, Dr. Fátima Guedes da Silva, and Lic. Natércia Martins for assistance in the electrochemical study. E.R. was supported by FWF (Austrian Science Fund) and University of Vienna (Faculty of Sciences and Mathematics, International Relations Office).

Supporting Information Available: X-ray crystallographic files in CIF format for **1** and **3**. Additional figures. This material is available free of charge via the Internet at http://pubs.acs.org.

IC034605I

(67) Jakupec, M. A. Unpublished results.